Heat-Transfer Enhancing Features for Handler Tray-Type Device Carriers

Andreas C. Pfahnl, John H. Lienhard, V, and Alexander H. Slocum

***Abstract*— Many test handlers process semiconductor devices in trays which must be rapidly heated or cooled by a forced air flow to a desired test temperature and then back to ambient temperature. This paper describes a new design feature for test-handler tray that significantly increases the rate of convective heat transfer to the tray and the devices in the tray. The improved tray incorporates lateral ribs which breakup thermal boundary layers and enhance mixing. This enhanced heat transfer is especially important in new test-in-tray handlers whose operating speeds can be limited by thermal response times.**

***Index Terms*— Device thermal response, heat transfer, heat-transfer enhancement, JEDEC carrier, test handler, thermal testing.**

NOMENCLATURE

Roman Symbols

A	Tray width, m.
$A_{c,\mathrm{air}}$	Duct airflow cross-sectional area, m^2.
$A_{c,\mathrm{tray}}$	Tray cross-sectional area, m^2.
B	Tray spacing, m.
b_1	Constant as defined by (14).
b_2	Constant as defined by (15).
c_{air}	Specific heat of air at constant pressure, J/kgK.
c_{tray}	Specific heat of the tray material, J/kgK.
D_h	Hydraulic diameter, m.
e	Tray rib height, m.
e^+	Roughness Reynolds number, (10).
f_{av}	Average friction factor.
f_s	Friction factor of a four-sided smooth duct.
f_r	Friction factor of a four-sided ribbed duct.
h_{av}	Average heat-transfer coefficient, W/m^2K.
L	Tray length, m.
P	Tray rib pitch, m.
P_{duct}	Duct perimeter, m.
Pr	Prandtl number of air.
Re_{Dh}	Reynolds number based on the hydraulic diameter.
$\mathrm{Re}_{2R\mathrm{av}}$	Reynolds number based on the average ray length, (8).
$\mathrm{St}_{\mathrm{av}}$	Average Stanton number.
St_s	Stanton number of a four-sided smooth duct.
St_r	Stanton number of a four-sided ribbed duct.
t	Time, s.
$T_{\mathrm{air,inlet}}$	Fixed inlet air temperature, °C.
$T_{\mathrm{air}}(x,t)$	Local, time-dependent air temperature, °C.
$T_{\mathrm{tray}}(x,t)$	Local, time-dependent tray temperature, °C.
V_{air}	Velocity of air, m/s.
x	Lengthwise position, m.

Greek Symbols

ΔP	Pressure drop, Pa.
ρ_{air}	Density of air, kg/m^3.
ρ_{tray}	Density of the tray material, kg/m^3.
v_{air}	Kinematic viscosity of air, m^2/s.
τ	Integration variable.

Manuscript received February 19, 1998; revised July 2, 1998.

A. C. Pfahnl is with Kinetrix, Inc., Bedford, NH 03110 USA (e-mail: andy.pfahnl@kmx.teradyne.com).

J. H. Lienhard and A. H. Slocum are with the Massachusetts Institute of Technology, Cambridge, MA 02139 USA (e-mail: lienhard@mit.edu; slocum@mit.edu).

Publisher Item Identifier S 1083-4400(98)09371-1.

I. INTRODUCTION

INTEGRATED circuit (IC) test handlers work with an electronics tester to automate the electrical testing of IC devices. The handler transports devices to and from the tester and must align and mechanically place the devices against the tester's interface. Handlers also heat or cool the devices, so that they can be tested at an elevated or depressed temperature (−60 °C to 160 °C).

A typical test handler has three main temperature-controlled zones. The first zone is a soak chamber in which devices are heated or cooled to the test temperature. The second zone is a test chamber, in which the devices are maintained at the test temperature while they are being tested. The last chamber is a desoak chamber in which the devices are returned to ambient temperature.

Many test handlers thermally condition (warm or cool) IC devices in special tray-type carriers known as boats. To minimize the device and tray thermal-response time and maximize the throughput (processing rate) of the test handler, a novel heat-transfer enhancing tray feature has been developed and implemented in the test tray of Kinetrix's In-Tray-Test handler. The design is based on heat-transfer augmentation in a two-ribbed-wall rectangular duct. Design equations are given which allow comparison of different tray designs. Experimental results are described that illustrate good agreement between the theoretical predictions and actual response. This concept can be applied to any handler type, test tray, or boat subject to a convective heating or cooling.

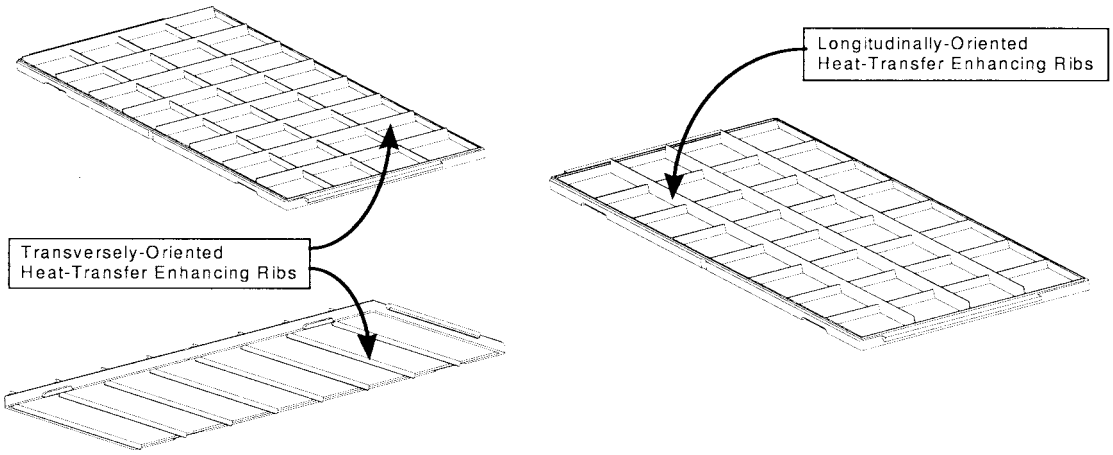

Fig. 1. Illustration of generic JEDEC-type trays having heat-transfer enhancing ribs.

II. Background

The throughput of a test handler at a high or low temperature can be limited by the time required to heat or cool the devices being tested. For forced air systems, this "soak" time is governed by the conditions of the airflow and the properties and geometry of the packaging. A turbulent airflow yields greater convective heat transfer. A higher conductivity device package helps improve the thermal response. However, because the ratio of the conductive thermal resistance to the convective thermal resistance (Biot Number) of most thin ($\sim$1 mm thick) plastic-packaged devices is less than one, the convective resistance usually controls the device thermal response. Because we have the freedom to design the layout of a test-handler tray, the approach taken here is to incorporate surface-roughening features on the tray which increase mixing in the airstream and reduce convective resistance. This design offers a compact and cost-effective means of enhancing the convective heat transfer for a given tray platform.

Past applications of rib augmentation have included the internal air cooling of turbine blades [9], [16], [17], the cooling of scram-jet engine inlets, electric utility steam condensers [18], nuclear-reactor fuel rods [4], and internal water cooling of turbine blades [12]. Most research on the subject of rib-roughened surfaces focuses on round ducts or pipes [4], [10], [11], [18]–[21]. The correlations and work based on circular geometries are commonly applied to other geometries by using the hydraulic diameter. More accurate results can be obtained from experimental measurements made directly on rectangular-shaped ducts.

One such study examined a wire transversely fastened to a surface of a rectangular duct [5]. Two other works [14], [15] investigated heat-transfer and pressure-drop performance of a wall populated with rectangular protuberances, representing integrated circuit (IC) devices on cards, opposite a smooth wall. Still others have considered transversely oriented ribs on the walls of a rectangular duct [1], [3], [6], [8], [12], [13], [22]–[24]. Transverse rib roughness is well suited to test-tray configurations and is the method of enhancement adopted in the present work. For our designs, the results of Han [7] are the most relevant. That work is described at length in a later section of this paper.

III. Integrally Ribbed Trays

The handler test tray considered here follows the general guidelines established by the Joint Electronic Device Engineering Council (JEDEC) for tray type carriers. JEDEC-standard trays have a network of tray ribs that define the pockets in which devices reside and that add structural stiffness to the tray. It minimizes the impact on the basic tray design if the existing structural ribs are also used as the thermal-enhancing ribs by simply increasing their heights above the top surface of the devices. The specific structural ribs to be used must be perpendicular to the direction of the airflow, most likely oriented down the length or across the width of the tray.

The trays depicted in Fig. 1 illustrate heat transfer enhancing ribs oriented in two different along a JEDEC-outline tray; the ribs can of course be applied to any custom or standard tray.

IV. Thermal Enhancement With Integrally Ribbed Trays

The flow traversing the tray should be turbulent in order to maximize cross-stream mixing and to raise the heat-transfer coefficient. To study and predict the thermal response of devices thermally conditioned in a tray, an engineering model must be developed that best represents the actual system. In the case considered here, the handler thermal-conditioning chambers vertically space a group of trays with the heat-transfer enhancing ribs on both top and bottom surfaces. Temperature-controlled air flows down the length of the tray. Vertical panels adjacent to the sides of the trays confine the flow laterally. In effect, the vertically-spaced trays form a series of ribbed, rectangular ducts whose width and length correspond approximately to the geometry of the tray: 13.59 cm (5.35 in) by 32.26 cm (12.7 in). The duct height is measured from the top surface of the devices in the tray to the underside of the pocket of the tray above. The duct height and width then allow a hydraulic diameter to be calculated

$$D_h = \frac{2AB}{A+B} \tag{1}$$

where A is the tray width and B is the tray spacing. The rib height, e, is measured from the top surface of the device

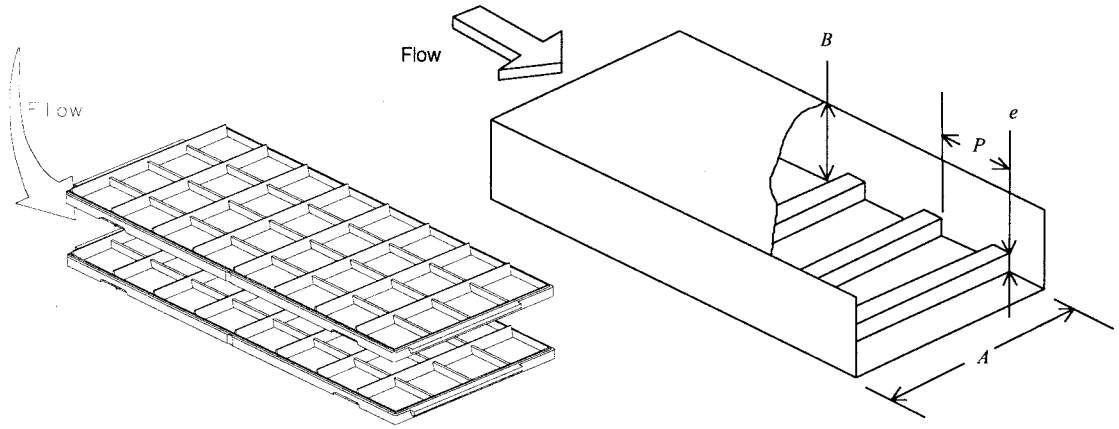

Fig. 2. Illustration comparing (a) two spaced JEDEC-type trays with (b) a two-sided ribbed duct.

to the top surface of the rib, and the rib pitch, P, is the center-to-center distance between successive ribs.

The diagrams in Fig. 2 show the similarity between the flow between two ribbed trays spaced vertically and a rectangular duct flow lined with ribs.

A. Pressure-Drop and Heat-Transfer Coefficient Design Equations

The work by Han [7] considers steady-state conditions, where a constant heat flux is applied along the length of the ribbed duct's section and a turbulent fully-developed airflow passes down the channel. Differences in heat transfer results may occur because a tray of chips does not provide a constant heat flux condition and the situation is transient; pressure drop measurements should agree well. Han's experiments were for Reynolds numbers between 7000 and 90 000. The different rib and duct geometries considered are described by the rib pitch-to-height (P/e) and the rib height-to-hydraulic diameter (e/D_h) ratios. The range considered in his work was $10 < P/e < 40$ and $0.021 < e/D_h < 0.063$.

The final design equations from Han's work allow the friction factor and Stanton number to be calculated. The average friction factor is given as a weighted average of the friction factor for a four-sided smooth duct and a four-sided ribbed duct

$$f_{\text{av}} = \frac{Af_s + Bf_r}{A+B}. \tag{2}$$

The smooth friction factor is iteratively calculated from

$$\frac{1}{\sqrt{f_s}} = 4.0\log_{10}\left(\text{Re}_{D_h}\sqrt{f_s}\right) - 0.40 + 4.0\log_{10}\left(\frac{1.156 + (B/A - 1)}{B/A}\right) \tag{3}$$

and the rough friction factor is calculated from

$$f_r = \frac{2}{\left[0.95(P/e)^{0.53} - 2.5\ln\frac{2e}{D_h} - 2.5 - 2.5\ln\frac{2B}{A+B}\right]^2}. \tag{4}$$

This last equation is developed from theoretical and prior experimental work as detailed in Han [7]. The pressure drop can then be calculated from the definition of the average friction factor (Fanning friction factor)

$$f_{\text{av}} = \frac{\Delta P}{4\left(\frac{L}{D_h}\right)\left(\frac{\rho_{\text{air}}V_{\text{air}}^2}{2}\right)} \tag{5}$$

where L is the length of the tray and V_{air} is the air velocity.

A similar approach is taken to calculate an average heat-transfer coefficient. An average Stanton number is calculated from the Stanton number for a four-sided smooth duct and from a four-sided ribbed duct having the same overall duct geometries

$$\text{St}_{\text{av}} = \frac{A\text{St}_s + B\text{St}_r}{A+B}. \tag{6}$$

The Stanton number for a duct with smooth surfaces is given by

$$\text{St}_s = \frac{0.023}{\text{Re}_{2R_{\text{av}}}^{0.2}\text{Pr}^{0.6}} \tag{7}$$

where the Reynolds number is based on an average "ray length" for improved accuracy

$$\text{Re}_{2R_{\text{av}}} = \left[\frac{D_h(1.156 + B/A - 1)}{B/A}\right]\frac{V_{\text{air}}}{\upsilon_{\text{air}}}. \tag{8}$$

The Stanton number for a duct with roughened walls is calculated using

$$\text{St}_r = \frac{f_r/2}{1 + \sqrt{f_r/2}\left[4.5(e^+)^{0.28}\text{Pr}^{0.57} - 0.95\left(\frac{P}{e}\right)^{0.53}\right]} \tag{9}$$

for e^+ greater than 25, where e^+ is defined as the roughness Reynolds number

$$e^+ = \frac{e}{D_h}\,\text{Re}\left(\frac{f_r}{2}\right)^{0.5}. \tag{10}$$

The restriction is that $P/e \geq 10$ and $e^+ \geq 35$. The derivation of these design equations is also described by Han [7]. The heat-transfer coefficient is then calculated using the definition of the Stanton number

$$h_{\text{av}} = \rho_{\text{air}}V_{\text{air}}c_{\text{air}}\text{St}_{\text{av}} \tag{11}$$

where ρ_{air} is the density of air, and c_{air} is the specific heat of air.

B. Thermal-Response Time Design Equations

We must now determine the device thermal response time or soak time. The soak time is a function of the device package material, package size, chip characteristics, and lead-frame characteristics. An enormous number of different chips exist yet a simple method is needed here for estimating the thermal response time of the devices residing in trays. The approach taken is to consider only the thermal resistance of the encapsulant material (our focus is on plastic packaging). For illustration, a thin small outline package (TSOP) 1.016-mm thick with a molding-compound thermal conductivity of 1.46 W/mK is considered. Even with a relatively high convective heat-transfer coefficient, say 100 W/m^{2}K, the Biot number remains well below unity. For other package types with larger Biot numbers, a more intricate analysis including the conduction resistance in the device package must be considered.

In a typical configuration, the airflow above the tray traverses a distance of as much as 30 cm. Heat loss to the devices gives rise to a temperature decrease in the air along the length of the tray. This gradient is initially large. Over time, it diminishes as the tray and its devices reach the inlet air temperature. Arpaci [2] gives a method for calculating the thermal response of a duct subject to a step change in the fluid temperature. The model is applied to the case at hand, where the trays of devices are modeled as the duct walls. In the analysis, the heat-transfer coefficient is assumed constant and uniform on all surfaces. There is no axial or length-wise conduction and the contributions of the ribs to the net surface area are ignored. The final design equations describing the tray and air temperatures as a function of time, t, and length-wise position, x, are (12) and (13), as shown at the bottom of the page, where $t^* = t - x/V_{\text{air}}$. The initial temperatures in those equations are zero, but they can be set to any value. The constants b_1 and b_2 are

$$b_1 = \frac{h_{\text{av}} P_{\text{duct}}}{\rho_{\text{air}} c_{\text{air}} A_{c,\text{air}}} \tag{14}$$

and

$$b_2 = \frac{h_{\text{av}} P_{\text{duct}}}{\rho_{\text{tray}} c_{\text{tray}} A_{c,\text{tray}}}. \tag{15}$$

Here, h_{av} is the heat-transfer coefficient, P_{duct} is the perimeter of the duct, $A_{c,\text{tray}}$ is a cross-sectional area of the tray, $A_{c,\text{air}}$ is the cross-sectional area of the duct opening, ρ_{tray} is density of the tray material, and c_{tray} is specific heat of the tray material. The properties of air are evaluated at the mean film temperature based on the initial temperature of the tray and the inlet temperature of the air. The tray is modeled as being made of a device encapsulant, which has the following thermal properties: $\rho_{\text{tray}} = 2070$ kg/m^3, $c_{\text{tray}} = 1170$ J/kgK.

V. Wind Tunnel Experiments

A wind tunnel (Fig. 3) was used to test the thermal response of devices in JEDEC-standard trays and to experimentally investigate the heat-transfer enhancing performance of different ribbed tray designs. The results were compared to the theoretical predictions. The wind tunnel uses a blower located at the head of the wind tunnel to provide an air flow, ball valves to vary the flow rate, and a venturi tube to measure the flow rate. A heater inside an aluminum tube warms the air to the desired test temperature before it enters the tray test chamber (Fig. 3).

The test chamber is instrumented with temperature and pressure sensors at the inlet and outlet positions. Two JEDEC-type trays can be placed inside the test chamber, one above the other. The lower tray rests on the edge of the JEDEC-type frame. The top tray is supported by the end tabs of the JEDEC-type frame, permitting JEDEC-conforming trays with different interior constructions to be examined at the same tray spacing. The wind tunnel is limited to air temperatures below 60 °C because of the PVC, wood, and other low-temperature components used in its construction.

A. Pressure-Loss Tests

In the tests, the pressure drop across the trays at different flow rates was obtained by adjusting the flow-control valve located after the venturi tube. At least ten different pressure drop readings were taken for each experiment. Two experiments were conducted on ribbed trays in order to establish the applicability of predictions using the method of Han [7] for JEDEC-type trays.

The first experiment uses a ribbed master tray made from aluminum. This tray has JEDEC-standard end tabs and a regular pattern of transversely oriented square ribs. When placed in the wind tunnel test section, the master-rib trays

$$T_{\text{tray}}(x,t) = \begin{cases} 0 & t < x/V_{\text{air}} \\ T_{\text{air,inlet}} b_2 e^{-b_1 \frac{x}{V_{\text{air}}}} \int_0^{t^*} e^{-b_2 \tau} I_0\left[2\left(\frac{b_1 b_2 x \tau}{V_{\text{air}}}\right)^{1/2}\right] d\tau & t \geq x/V_{\text{air}} \end{cases} \tag{12}$$

and

$$T_{\text{air}}(x,t) = \begin{cases} 0 & t < x/V_{\text{air}} \\ T_{\text{air,inlet}} e^{-b_1 \frac{x}{V_{\text{air}}}} \left\{ \begin{aligned} & e^{-b_2 t^*} I_0\left[2\left(\frac{b_1 b_2 x \tau}{V_{\text{air}}}\right)^{1/2}\right] \\ & + b_2 \int_0^{t^*} e^{-b_2 \tau} I_0\left[2\left(\frac{b_1 b_2 x t^*}{V_{\text{air}}}\right)^{1/2}\right] d\tau \end{aligned} \right\} & t \geq x/V_{\text{air}} \end{cases} \tag{13}$$

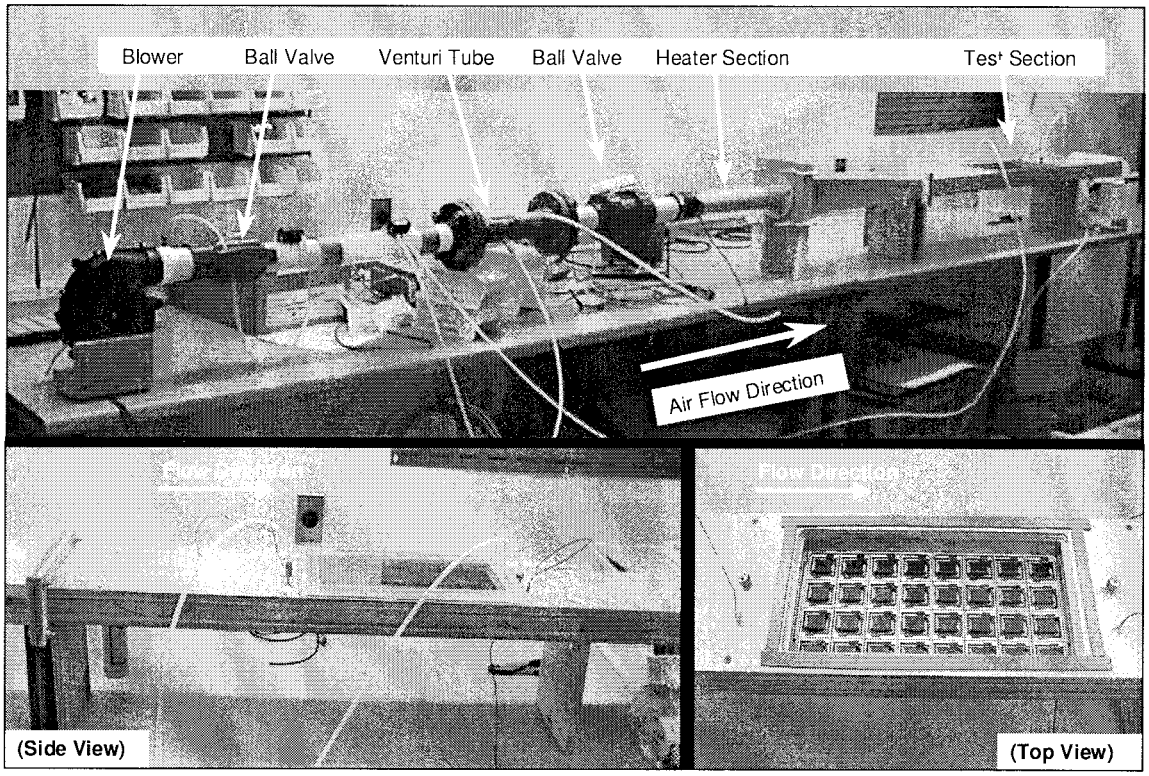

Fig. 3. The complete wind tunnel is shown in the top picture and the test section is shown in the bottom picture.

are 13.59 cm (5.35 in) wide and spaced 23.62 cm (0.93 in) apart, which is taken as the tray spacing or duct height. The resulting hydraulic diameter is 4.01 cm (1.58 in). The pitch of the ribs is 2.84 cm (1.12 in) and the width of each rib is 0.343 cm (0.135 in). Moreover, each one of the 11 ribs is 0.343 cm (0.135 in) tall. The resulting e/D_h ratio is 0.085 and the P/e ratio is 8.3. This idealized tray geometry is found to have excellent agreement with the pressure-loss correlations of Han [7], even though the experiment falls somewhat outside the bounds on his parameters.

The second experiment on ribbed trays is with an actual handler test tray (Kinetrix's flex-insert tray) shown in Fig. 4. This tray has a series of ribs extending high above the device surfaces and beyond the underside of the insert surfaces. The ribs are slightly staggered to allow other identical trays to stack on it. Fig. 4 shows top and bottom views of the tray.

The top photograph of Fig. 4 shows more clearly how the top ribs extend beyond the top of the JEDEC-type frame. The ribs are at a 3.89 cm (1.53 in) pitch and extend 0.38 cm (0.15 in) above the top surface of the flex insert. The underside view of the tray shows how the inserts are recessed deep into the tray. The bottom ribs are flush or in line with the bottom edge of the frame, in order that they can be easily accepted into other, already existing, manufacturing machines (e.g., lead inspection and marking machines). It was possible to make the distance from the bottom of the tray to the bottom of the flex insert, i.e. the rib height, identical to that of the top side, namely 0.38 cm (0.15 in). When placed inside the test section of the wind tunnel, the tray spacing is 2.49 cm (0.98 in), yielding a hydraulic diameter of 4.19 cm (1.65 in). The resulting e/D_h ratio is 0.097 and the P/e ratio for either side is 9.6. The resulting pressure-drop data gathered over a similar flow-rate and Reynolds-number range (2 500 to 19 000) as the previous experiments is shown in Fig. 5 and is plotted against predictions.

The results of the pressure drop experiments on Kinetrix's flex-insert tray show excellent agreement with predictions. The pressure losses are under 20 Pa (0.08 in H_2O) in the expected flow-rate range of 4.72×10^{-3} m^3/s (10 CFM) to 9.44×10^{-3} m^3/s (20 CFM), which is not large compared to typical losses in the air handling system. With confirmation that the method of Han [7] can predict the pressure losses, the design equations presented earlier can be used to evaluate the impact changes in the tray spacing, rib height, and rib pitch might have on the pressure losses.

B. Heat-Transfer Tests

The thermal response of TSOP devices residing in two different types of trays was measured. Temperature data was obtained using thermocouple-instrumented TSOP devices located in the trays being investigated. The wind tunnel was warmed to about 50 °C and then a fully-populated ambient-temperature tray was quickly inserted into the wind tunnel, while maintaining a fixed inlet air temperature and fixed velocity air flow. A temperature controller maintains the inlet air temperature fixed to within 1.0 °C.

The first tray design tested is Kinetrix's handler test tray shown earlier. The tray placed in the lower position of the wind tunnel test section is populated with 44-lead TSOP-II devices with no internal chips (dummy devices). The package

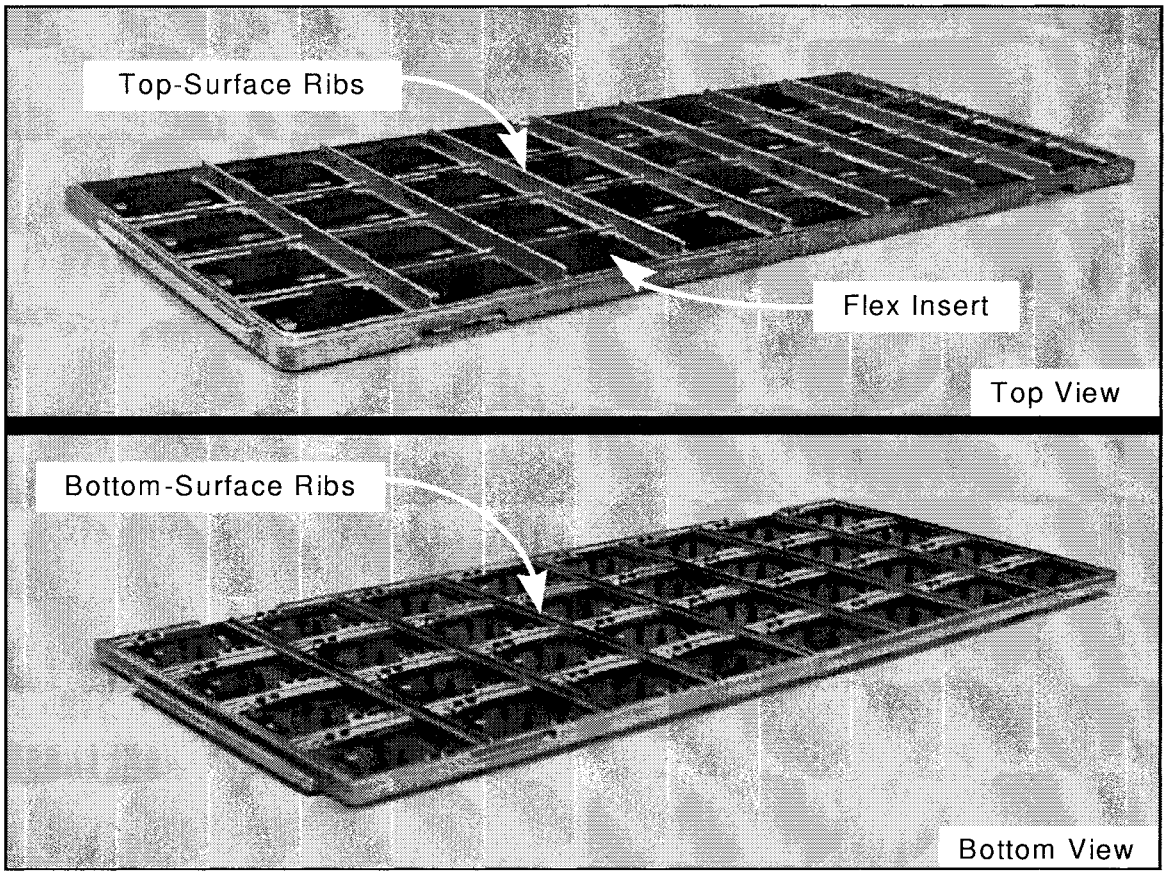

Fig. 4. Photographs of the top and bottom surfaces of the Kinetrix's 32-site flex-insert trays showing the heat-transfer enhancing rib structures.

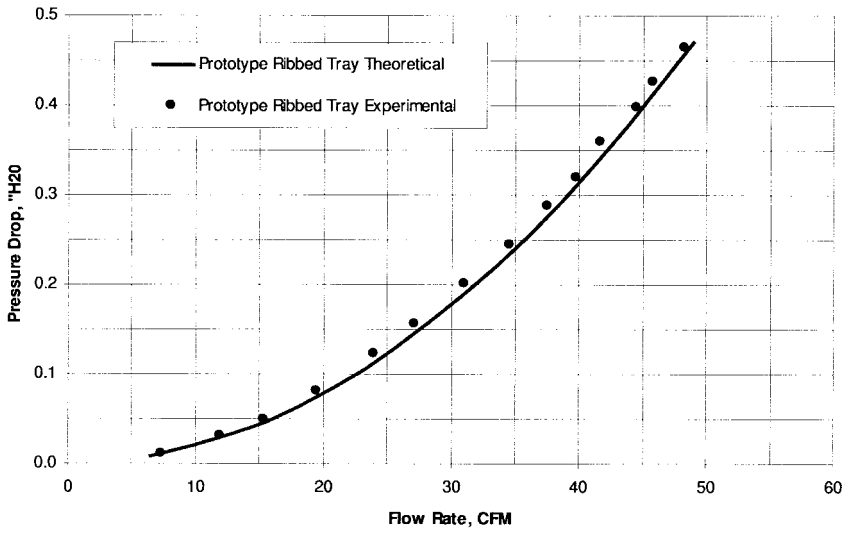

Fig. 5. Experimental pressure-drop results for a ribbed test tray (shown in Fig. 4) compared with the predicted pressure losses.

of these devices is 1.016 mm thick. Small 0.1 cm (0.04 in) diameter holes were drilled through the center of the first and last pocket insert of the second column. This exposed a very small section of the underside of the devices. T-type 0.0127 cm (0.005 in) wire-diameter thermocouples were epoxied in place. The thermocouple-instrumented tray was in the bottom position. The results are shown in Fig. 6 for a flow rate of 7.08×10^{-3} m^3/s (15 CFM) or $\mathrm{Re}_{D_h} \approx 7{,}400$ and in Fig. 7 for 22.65×10^{-3} m^3/s (48 CFM) or $\mathrm{Re}_{D_h} \approx 15{,}000$.

The thermal-response results agree well with the predictions. The experimental and theoretical results differ in both cases by only a few degrees during the transient region. The difference is likely attributable to the imperfect adiabatic boundary condition offered by the wind tunnel walls. Given these good

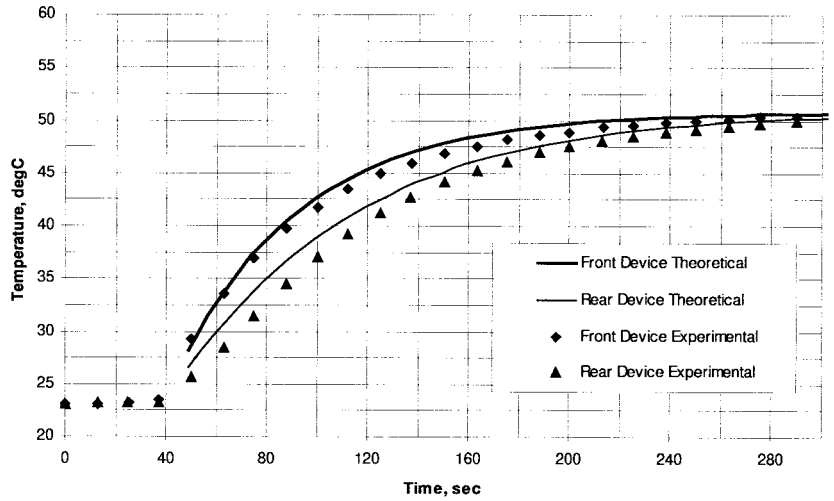

Fig. 6. Temperature response of devices carried in Kinetrix's flex-insert tray when suddenly exposed to a 51 °C airflow at 7.08×10^{-3} m^3/s (15 CFM).

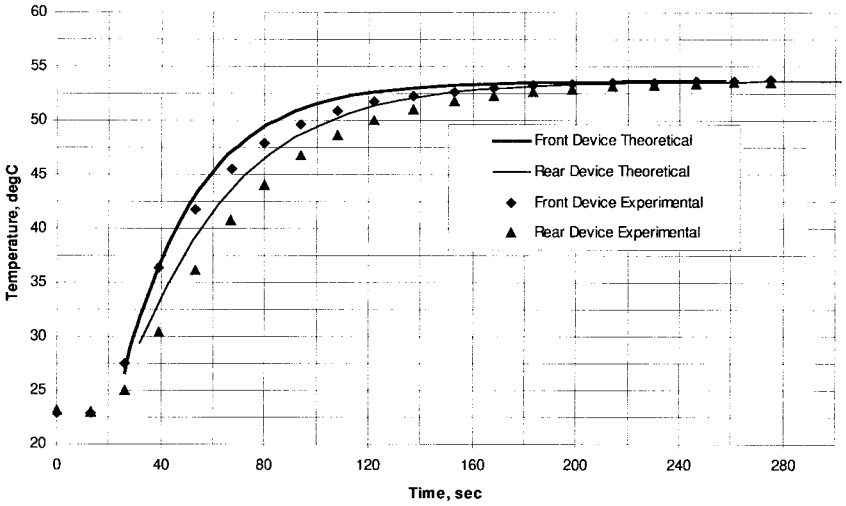

Fig. 7. Temperature response of devices carried in Kinetrix's flex-insert tray when suddenly exposed to a 53 °C airflow at 22.65×10^{-3} m^3/s (48 CFM).

predictions of the tray and device thermal response, the design equations presented earlier can reasonably be used to evaluate the impact changes in the tray spacing, rib height, and rib pitch might have on the thermal response.

To demonstrate the actual enhancement of the ribs, the same tests were performed on a standard TSOP process tray (Fluoroware P/N 40026-07-116-8) which has no enhancements. In this tray, the first and last devices of the third column are instrumented with thermocouples. Because a device sits in the tray with its underside exposed, the thermocouples were epoxied directly to the devices without drilling first through the tray. The thermocouple-instrumented tray is again placed in the lower position of the test section and an empty one is placed in the upper position. The results of this experiment are shown in Fig. 8.

Thermal response time for the filled TSOP process tray is approximately 560 s which is much greater than that of Kinetrix's ribbed flex-insert tray at the same flow rate: to achieve the same temperature rise, the process tray requires 2.5 times longer to warm to within 1 °C of the final temperature. Clearly, the throughput of test-in-tray type handlers can be dramatically improved using a high thermal performance tray. Similar results were found at a flow rate of 21.24×10^{-3} m^3/s (45 CFM) with these two trays. Experiments, however, have not been completed to determine the level of improvement offered by ribs on other test or process trays (e.g., custom non-JEDEC types), although similar performance enhancements can be expected.

VI. Conclusion

This paper describes the design, analysis, and testing of the heat-transfer performance of an enhanced tray-type IC carrier used in a semiconductor test handler. Novel design features in the form of ribs are introduced to improve the thermal response time of devices in these carriers. Reducing the thermal response time of the devices in a test-handler tray allows reduction of the size of the thermal-conditioning chambers in the handler. Moreover, this improved thermal response makes it possible to reach the very high throughputs found in new test-in-tray type handlers, for which throughput is not limited by the pick-and-place operations of old-style handlers that would normally outweigh the soak time. Finally,

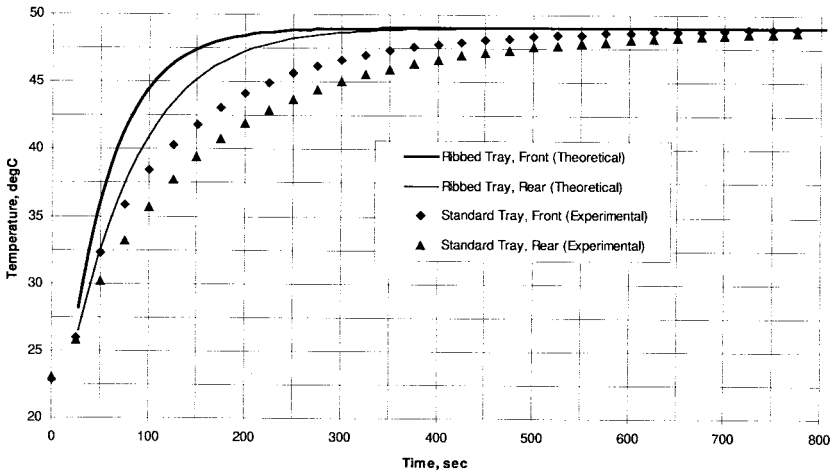

Fig. 8. Temperature response of devices carried in a process tray when suddenly exposed to a 49 °C airflow at 9.91×10^{-3} m^3/s (21 CFM).

the features help minimize the required airflow rate. Very high airflow rates lead to greater noise, higher total pressure drops, and higher component (e.g. blower) costs. Kinetrix has applied for patents on key features of this design.

Experimental testing with a wind tunnel was used to compare the thermal response of different trays. Furthermore, the experimental pressure-drop and heat-transfer results from tests on a ribbed tray are in good agreement with theoretical predictions. The rib height and airflow rate have the greatest impact on the tray and device thermal response.

The performance increases discussed in the heat-transfer sensitivity study must be put into perspective. A decrease in the thermal response time does translate to an increase in a handler throughput. However, the airflow system operating point will be affected by the increased pressure drop of rib enhancements, and so a complete analysis must obviously consider the blower and ducting.

REFERENCES

[1] S. Aiba, "Heat transfer around small square ribs mounted on an adiabatic plane channel," *Waerme-und Stoffuebertragung*, vol. 25, pp. 85–91, 1990.

[2] V. S. Arpaci, *Conduction Heat Transfer*. Reading, MA: Addison-Wesley, 1966, pp. 354–357.

[3] F. Burggraf, "Experimental heat transfer and pressure drop with two-dimensional discrete turbulence promoters applied to two opposite walls of a square tube," in *Augmentation of Convective Heat and Mass Transfer*. New York: ASME: 1970, pp. 70–79.

[4] M. Dalle and L. Meyer, "Turbulent convection heat transfer from rough surfaces with two-dimensional ribs," *Int. J. Heat Mass Transf.*, vol. 22, pp. 583–620, 1979.

[5] E. J. Edwards and N. Sheriff, "The heat transfer and friction characteristics for forced convection air flow over a particular type of rough surface," in *International Developments in Heat Transfer, Part II*. New York: ASME, 1961, pp. 415–426.

[6] W. B. Hall, "Heat transfer in channels having rough and smooth surfaces," *J. Mech. Eng. Sci.*, vol. 4, no. 3, pp. 287–291, 1962.

[7] J. C. Han, "Heat transfer and friction in channels with two opposite rib-roughened walls," *J. Heat Transf.*, vol. 106, pp. 774–781, Nov. 1984.

[8] J. C. Han *et al.*, "An investigation of heat transfer and friction for rib-roughened surfaces," *Int. J. Heat Mass Transf.*, vol. 21, pp. 1143–1156, 1978.

[9] D. K. Hennecke, "Turbine blade cooling in aero engines—Some new results, future trends, and research requirements," *Studies in Heat Transfer*, J. P. Hartnett *et al.*, Eds. New York: Hemisphere, 1979.

[10] M. J. Lewis, "An elementary analysis for predicting the momentum and heat transfer characteristics of a hydraulically rough surface," *J. Heat Transf.*, vol. 97, pp. 249–254, 1975.

[11] ———, "Optimizing the thermohydraulic performance of rough surfaces," *Int. J. Heat Mass Transf.*, vol. 18, pp. 1243–1248, 1975.

[12] D. E. Metzger *et al.*, "Heat transfer and flow friction characteristics of very rough transverse ribbed surfaces with and without pin fins," in *Proc. 1983 ASME-JSME Thermal Eng. Conf.*, 1983, vol. 1, pp. 429–436.

[13] R. H. Norris, "Some simple approximate heat transfer correlations for turbulent flow in ducts with rough surfaces," in *Augmentation of Convective Heat and Mass Transfer*. New York: ASME, 1970, pp. 16–26.

[14] E. M. Sparrow, J. E. Neithammer, and A. Chaboki, "Heat transfer and pressure drop characteristics of arrays of rectangular modules encountered in electronic equipment," *Int. J. Heat Mass Transf.*, vol. 25, no. 7, pp. 961–973, 1982.

[15] E. M. Sparrow and D. R. Otis, Jr., "Ductflow heat transfer at a smooth wall which faces a wall covered by protuberances," *Int. J. Heat Mass Transf.*, vol. 28, no. 7, pp. 1317–1326, 1985.

[16] M. Suo, "Turbine cooling," in *Aerothermodynamics of Aircraft Gas Turbine Engines*, G. Oates, Ed. Wright-Patterson Air Force Base, OH: Air Force Aero Propulsion Lab., 1978, pp. 19–1 to 19–23.

[17] J. R. Taylor, "Heat transfer phenomena in gas turbine," *ASME*, no. 80-GT-172, 1980.

[18] R. L. Webb, "Toward a common understanding of the performance and selection of roughness for forced convection," in *Studies in Heat Transfer: A Festschrifft for E. R. G. Eckert*, J. P. Hartnett *et al.*, Eds. Washington, D.C.: Hemisphere, 1979, pp. 257–272.

[19] R. L. Webb, E. R. G. Eckert, and R. J. Goldstein, "Generalized heat transfer and friction correlations for tubes with repeated-rib roughness," *Int. J. Heat Mass Transf.*, vol. 15, pp. 180–184, 1972.

[20] ———, "Heat transfer and friction in tubes with repeated-rib roughness," *Int. J. Heat Mass Transf.*, vol. 14, pp. 601–617, 1971.

[21] R. L. Webb, L. L. Haman, and T. S. Hui, "Enhanced tubes in electric utility steam condensers," *Heat Transfer in Heat Rejection Systems*, S. Sengupta and Y. F. Mussalli, Eds. New York: ASME, 1984, vol. 37, pp. 17–26.

[22] D. Wilkie, "Forced convection heat transfer from surfaces roughened by transverse ribs," in *Proc. 3rd Int. Heat Transfer Conf.*, 1966, vol. 1, pp. 1–19.

[23] D. Wilkie *et al.*, "Friction factor measurements in a rectangular channel with walls of identical and nonidentical roughness," *Int. J. Heat Mass Transf.*, vol. 10, pp. 611–621, 1967.

[24] T. Yanagida *et al.*, "Heat transfer from a longitudinal row of heat dissipating rectangular bodies," *Trans. JSME*, vol. 54, pp. 1294–1301, 1984.

Andreas C. Pfahnl received the B.S. degree in mechanical engineering from Rensselaer Polytechnic Institute, Troy, NY, in 1992 and the M.S. and Sc.D. degrees in mechanical engineering from the Massachusetts Institute of Technology, Cambridge, in 1995 and 1998, respectively.

Over the past six years, he has worked and consulted for various companies in the semiconductor industry. For the past two years, he has been working for Kinetrix Inc., Bedford, NH. His main interests are in thermal design of manufacturing equipment.

John H. Lienhard, V received the B.S. and M.S. degrees from the University of California at Los Angeles, both in thermal engineering, and the Ph.D. degree in applied mechanics from the University of California, San Diego, in 1988.

He joined the Department of Mechanical Engineering, Massachusetts Institute of Technology, Cambridge, in 1988, where he is an Associate Professor in the Rohsenow Heat and Mass Transfer Laboratory. His research interests are in heat transfer, electronics temperature control, high heat flux engineering, convective cooling, and thermal manufacturing processes. He consults extensively in the electronics and manufacturing industries.

Dr. Lienhard received the NSF PY1 Award, the SAE Teetor Award, an ASME Best Paper Award, the R&D 100 Award, and several teaching awards.

Alexander H. Slocum received the Ph.D. degree in mechanical engineering from the Massachusetts Institute of Technology (MIT), Cambridge, in 1985.

He was with the National Institute of Standards and Technology, Gaithersburg, MD, for three years. He joined the Mechanical Engineering Department, MIT, in 1991 where he is currently the Alex and Brit d'Arbeloff Professor of Mechanical Engineering. His research interests include the development of precision machines and components. He collaborates closely with industry to address relevant fundamental problems.

Dr. Slocum has received numerous patents and design awards.